Mineral. Deposita 24, 100–110 (1989)

MINERALIUM DEPOSITA

Sediment geochemistry and base metal sulphide mineralisation in the Quidong Area, southeastern New South Wales, Australia

K. G. McQueen

School of Applied Science, Canberra College of Advanced Education, P.O. Box 1, Belconnen A.C.T, 2616, Australia

Abstract. Geochemically anomalous, pyritic sediments occur directly above a Mid Silurian unconformity in the Quidong area of southeastern New South Wales. The composition of these sediments reflects derivation from a mixture of: (a) feldspar- and mica-depleted detritus reworked from underlying quartz-rich flysch; (b) Mg-rich clay or chlorite precipitated from hydrothermal exhalations; and (c) pyrite formed by reaction of iron in clays or oxides with reduced sulphur derived largely from sea-water sulphate and possibly a magmatic source. Three types of base metal sulphide mineralisation occur at Quidong including: (a) weak syngenetic concentrations in the pyritic sediments; (b) stratabound and fault-controlled bodies of massive sulphides hosted by the pyritic sediments and containing higher grade Pb, Zn and Cu; and (c) small vein and cavity fillings of galena, barite and other minor sulphides in overlying limestones. All types of mineralisation are related to hydrothermal activity which occurred during and after deposition of the pyritic facies. The geochemistry of the immediately underlying basement rocks and Pb isotope data indicate that the source of the metal-bearing fluids was deeper in the crust and probably related to widespread partial melting and magmatic processes. The sulphidic sediments and stratabound sulphide deposits represent syngenetic-epigenetic, sediment hosted mineralisation developed in a shallow marine environment, distal from major volcanic centers. This style of mineralisation has not previously been described from the region. It has some similarities to the Irish-Alpine type spectrum of deposits best known in Europe.

The Quidong basin in southeastern New South Wales contains Late Silurian, shallow marine sediments unconformably overlying a basement of Early Silurian flysch. Pyritic siltstones showing anomalous base metal and major element geochemistry occur at the base of the Late Silurian sequence directly above the unconformity. Stratabound and fault-controlled pyritic sulphide bodies, containing base metals, have also been discovered within these rocks and in parts of the overlying limestones. Although the known sulphide deposits appear to be too small for economic orebodies, they suggest the presence of a previously unrecognised style of sediment hosted mineralisation in the shallow marine parts of the Silurian volcanosedimentary sequences of the Lachlan Fold Belt in southeastern Australia.

This paper describes the petrology and geochemistry of the pyritic sediments and associated sulphide bodies and compares their geochemistry with that of the enclosing rocks. Using this information, together with isotopic data, a model is developed for the origin of the pyritic sediments and the base metal sulphide mineralisation at Quidong.

Geological setting

In the Quidong area, Silurian rocks occur in a fault-bounded, synclinal outlier within Late Ordovician sandstones and phyllites (Fig. 1). These Silurian rocks represent the southern extremity of the Cowra-Yass synclinorial zone in New South Wales (Scheibner 1973) and include Early to Middle Silurian flysch-type sediments (Tombong Beds and Merriangaah Siltstone) and an overlying Late Silurian sequence of shallow marine limestones, sandstones, siltstones and shales (Brunker et al. 1971, Crook et al. 1973). The Late Silurian sediments occupy a structural basin and have been subdivided into a limestone-rich unit (Quidong Limestone) and an overlying shale-rich unit (Delegate River Mudstone, Brunker et al. 1971, Pogson 1972, Fig. 2). The Quidong Limestone can be further subdivided into three separate but gradational facies, including a basal, pyritic facies, a massive and thick bedded limestone facies and an overlying thinly interbedded limestone-shale facies.

The Late Silurian sequence is stratigraphically equivalent to similar sediments at Yass, 230 km to the north (Link 1970, Pogson 1972), and broadly time equivalent to felsic volcanic rocks and associated sediments in the Canberra-Cooma region and in the Captain's Flat Synclinorial Zone to the north and north east respectively (Richardson 1979, Pickett 1982). The nearest felsic volcanic rocks of proximal type, and of likely Late Silurian age, occur in a small infaulted block 20 km north of Quidong.

The Silurian rocks at Quidong have been folded into mostly broad, open folds with NW to NE trending axes showing plunge reversals due to gentle cross folding. Intense faulting accompanied or followed this folding resulting in numerous high angle thrust faults which particularly disrupt the Late Silurian sequence. Mineral assemblages in the shales indicate only very low grade regional metamorphism. The immediately underlying Ordovician rocks show low greenschist facies grade metamorphism, but 6 km to the east this increases to amphibolite facies grade in a narrow metamorphic belt known as the Cambalong Complex (McQueen et al. 1986).

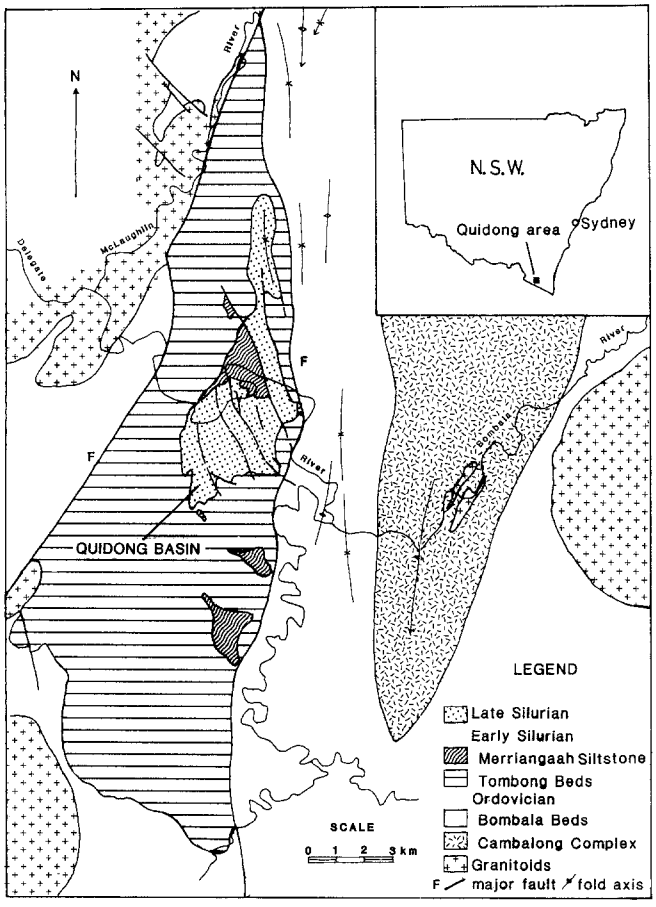

Fig. 1. Location and geological setting of the Quidong area in southeastern New South Wales

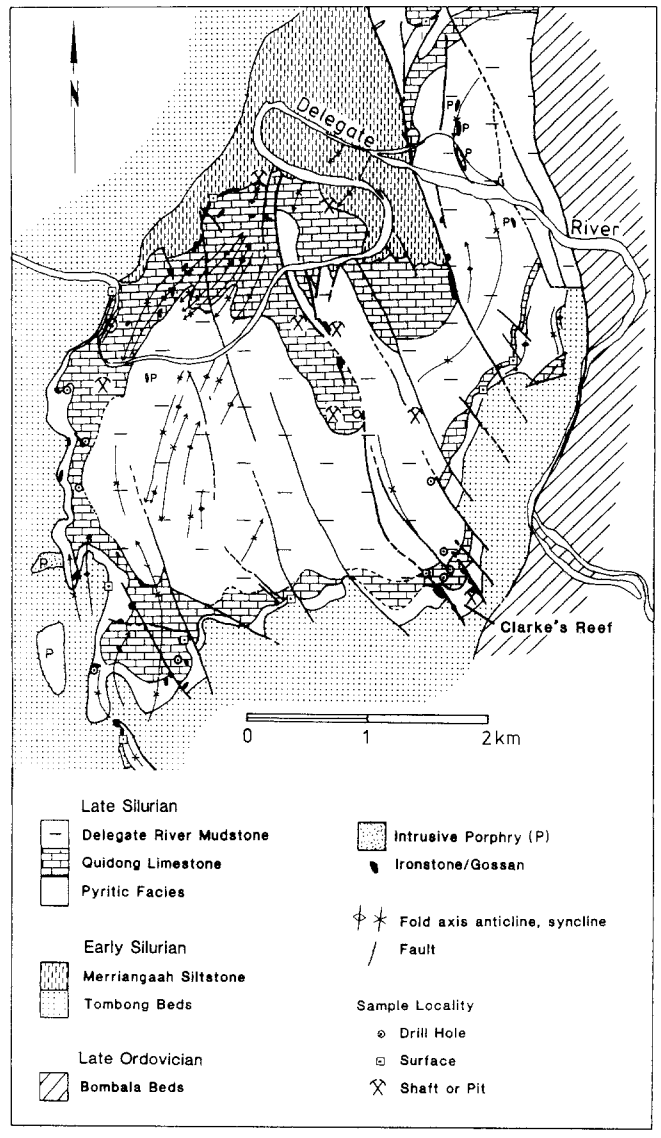

Fig. 2. Detailed geology of the Quidong Basin also showing location of sample sites

Porphyry dykes (quartz-feldspar-hornblende ± biotite) intrude both Silurian sequences at Quidong and are probably related to larger Siluro-Devonian granitoid intrusions in the surrounding area. The dykes are extensively altered (chloritised and epidotised) and exhibit much of the deformation recorded in the surrounding rocks. Some are also marked by narrow (<1 m) skarn zones where they intrude limestones.

Nature of the pyritic sediments

Highly pyritic sediments are restricted to the base of the Quidong Limestone and show their thickest development (up to 100 m) along the western, southwestern and southeastern margins of the basin (Fig. 2). Some weakly pyritic beds also occur within the overlying limestone-rich facies and rarely in the Delegate River Mudstone.

The pyritic facies is dominated by grey, quartz-rich and green chloritic siltstones, with minor calcareous siltstones. Sedimentary structures include small scale interbeds of sandstone and shale, plane lamination, graded bedding and minor soft sediment features such as load structures, contorted bedding, shale intraclasts and compacted bedding around fossil fragments. The siltstones consist largely of poorly sorted, subangular to subrounded detrital quartz grains (25–80%) with intergranular, matted chlorite (10–60%). Minor pyrite (up to 10%) is ubiquitous and some siltstones are very pyritic with up to 40% pyrite (Fig. 3a). Trace chalcopyrite, sphalerite and galena occur widely and are more abundant in some sulphide-rich sections. Other minor constituents include carbonate, rutile, zircon, and in some rocks, sericite and detrital plagioclase. Some dark siltstones also contain thread-like aggregates of organic carbon or graphite. There has been considerable post-depositional recrystallisation and solution activity in the siltstones. Quartz grains typically show secondary overgrowths and much of the chlorite has been recrystallised into coarse fibrous aggregates. Secondary veining by quartz, chlorite, sulphides and carbonate (mainly dolomite and siderite) is common and there has been some silicification and sulphide replacement of bioclastic carbonate material (Fig. 3c). Chlorite occurs in several texturally distinct forms, including a common pale green to yellowish variety in patchy aggregates, a fibrous type nucleated on pyrite, and platey or fibrous vein chlorite. Microprobe analyses of chlorites indicate generally Mg-rich compositions (clinochlore to pycnochlorite, Deer et al., 1967). In sulphide-rich

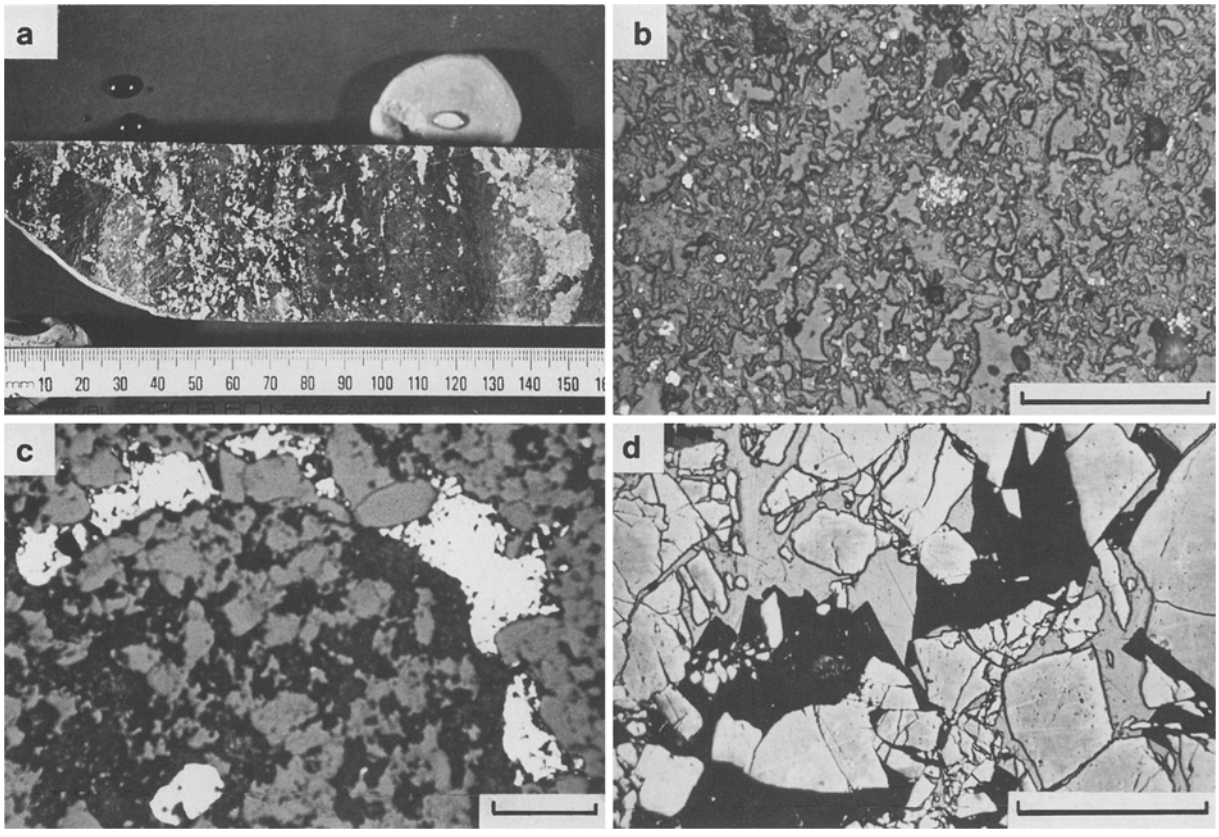

Fig. 3. **a** Drill core sample of pyritic siltstone from the pyritic facies at Quidong. **b** Photomicrograph of weakly pyritic, chloritic siltstone showing small clusters of framboidal pyrite. **c** Photomicrograph showing chalcopyrite replacement of brachiopod shell in silicified limestone from the top of the pyritic facies. **d** Photomicrograph of sample from massive ore zone at Clarke's Reef showing galena infilling and partially replacing fractured pyrite. All photomicrographs taken in plane polarised reflected light. Scale bars are 0.2 mm

sediments the intergranular chlorite is more Mg-rich, with a lower Fe content than chlorite from siltstones with lesser pyrite. Vein chlorite associated with massive sulphides is also a Mg-rich, lower Fe variety.

Shales interbedded with the siltstones consist of fine grained-chlorite, sericite and minor quartz with varying amounts of pyrite. Minor chalcopyrite and sphalerite occur with bedded pyrite and in cross-cutting pyrite- and quartz-rich veinlets. Some shale beds contain abundant benthonic fossils including various brachiopods, trilobites and corals.

Minor quartz-rich sandstones containing intergranular chlorite, minor pyrite and chalcopyrite, occur as thin (<5 cm) lenses within the siltstones, and less commonly as massive layers up to half a meter thick.

Carbonate-rich rocks, including dark biomicrites, coarse-to fine-grained bioclastic limestones and recrystallised, mottled limestones, are a minor component of the pyritic facies but increase in abundance towards the upper gradational boundary with the overlying limestone facies. These have a high terrigenous component and are also noticeably pyrite deficient, particularly where they contain abundant fossil fragments. Limestones throughout the sequence show evidence of extensive solution activity including stylolite development, nodular recrystallisation and dolomitisation. Calcite is the main carbonate but dolomite and siderite are also common, particularly in secondary veins and areas adjacent to faults.

Several thin (<0.6 m) beds of fine-grained tuff were intersected in drill core at the southern end of the basin. These contain irregular lithic fragments (<0.4 mm across) in a very fine-grained sericite-quartz matrix. Layers of cherty exhalite, composed of microcrystalline quartz, albite, minor chlorite and sericite, with trace pyrite and ilmenite, also occur lower in the sequence in the same area.

Sulphide mineralisation

Three types of sulphide mineralisation occur in the Quidong basin comprising: (a) weak stratiform mineralisation in the pyritic sediments; (b) stratabound and fault-controlled bodies of massive and semi-massive sulphides containing higher grade Pb, Zn and Cu concentrations; and (c) small vein and cavity fillings of galena and barite in limestones.

Stratiform sulphides

Stratiform mineralisation consists mainly of pyrite with minor to trace amounts of chalcopyrite, sphalerite and galena. The sulphides occur disseminated in bedding-parallel bands and in coarser grained sulphide-rich layers. The disseminated sulphides contain several different pyrite forms including framboids, tiny euhedral grains and clusters (<0.02 mm), and larger (0.2–2 mm) subhedral grains (Fig. 3b). Larger grains commonly show microfracturing,

pull-apart structures and pressure fringes of fibrous quartz and carbonate, suggesting that they crystallised before deformation of the enclosing rocks. Chalcopyrite, sphalerite and galena occur as inclusions in pyrite aggregates and less commonly as tiny irregular grains. Chalcopyrite also occurs in larger disseminated blebs (up to 5 mm across) and in replaced fossil fragments. Highly sulphidic sediments contain numerous lenses of coarse-grained pyrite as well as irregular, discordant pyrite veins. Pyrite forms include large cubes and pyritohedron (up to 2 cm), elongate, blade-like aggregates and irregular masses of subhedral grains (Fig. 3a). Some of the pyrite is skeletal and poikiloblastic and larger grains show growth zoning marked by silicate inclusions. Minor sphalerite, chalcopyrite and galena typically occur as irregular aggregates or fracture-filling veins in this pyrite. Small concretion-like structures of pyrite, chalcopyrite and carbonate are also present in some sandy units.

Massive and vein-type sulphides

Irregular bodies of massive to semi-massive sulphide (up to 9 m thick) occur within the pyritic facies, outcropping as rubbly ironstone masses in areas of faulting. Large veins of similar material also extend along faults into the adjacent and overlying limestones. Some of these deposits were mined on a small scale in the 1860s and 1870s. More recent drilling by Esso Australia Ltd. (1971–1972), Western Mining Corporation Pty Ltd. (1981–1983) and Plagoldmin Pty Ltd. (1985) has tested a number of targets in the pyritic facies and delineated the Clarke's Reef prospect on the southeastern edge of the basin (Fig. 2).

The Clarke's Reef prospect occurs within thick, pyritic sediments in an intensely faulted and north plunging, graben-like structure. This structure lies on a northwest trending zone of major faulting, the northeast margin of which appears to have been a basin high at the time of deposition. Faults along the zone extend into the Ordovician basement. At surface, the Clarke's Reef area is marked by numerous outcrops of massive gossan and ferricrete, as well as ferruginous, weathered sediments and soils. Pronounced Pb, Zn and Cu anomolies have been detected in the soils. Massive barite also outcrops at the surface. The distribution of ferruginous outcrops, and of massive pyritic material in drill core, suggest that the mineralisation is broadly stratabound but with some discordant and fault-controlled massive veins. Drilling has indicated that these sulphide-rich zones contain up to 9.7% combined Cu, Pb and Zn over intervals of up to 7 m (Brooke 1981). The massive sulphides consist mainly of coarse-grained and brecciated pyrite showing growth zoning, as well as skeletal and colloform textures. Sphalerite, galena and, in some sections, chalcopyrite occur as an infilling matrix, as irregular intergranular aggregates, or as vein fillings in the pyrite (Fig. 3d). Small inclusions of galena and chalcopyrite commonly show crystallographic control by the enclosing pyrite. Textures in some of the veins indicate replacement of pyrite by the other sulphides. Massive sulphides at Clarke's Reef also locally contain abundant monoclinic pyrrhotite enclosing and partially replacing subhedral grains and bladded aggregates of pyrite. Microscopic observation reveals large, smooth pyrite relicts rimmed by porous, granular pyrite with irregular magnetite inclusions. This pyrite-magnetite mixture appears to have replaced pyrrhotite around the relicts of earlier pyrite. Minor chalcopyrite is present as fracture-fillings in the relict pyrite and as inclusions in pyrrhotite. These various textures suggest a complex history of sulphide development involving early formation of coarse crystalline pyrite, deformation of massive pyrite, introduction or remobilisation of sphalerite, galena and fracture-filling chalcopyrite, localised replacement of pyrite by pyrrhotite, followed by oxidation of pyrrhotite to pyrite and magnetite.

Microprobe analyses of pyrite and pyrrhotite from Clarke's Reef reveal low Ni and Co contents (generally below detection, Table 1). Separate wet chemical analyses of 13 pyrite samples indicate 5–460 ppm Co and 5–90 ppm Ni, suggesting concentration of Co relative to Ni in some of the pyrite. Trace amounts of As (up to 0.21%) are present in the iron sulphides. Sphalerite from Clarke's Reef is a low-Fe variety (3.1 mol% FeS) and the galena contains little or no Ag or Sb (Table 1).

The gangue component to this mineralisation consists of brecciated, veined and recrystallised host rock material, milky and crystalline quartz, chlorite, dolomite, siderite, minor barite and calcite.

Galena and barite in limestones

Some irregular and vein-like bodies of fracture-filling galena and barite occur in limestones overlying the pyritic facies rocks. This mineralisation is generally associated with faults or permeable zones, is typically vughy and composed of coarse-grained galena and barite in a dolomite-rich gangue. Minor chalcopyrite, sphalerite, pyrite and quartz also occur in some parts. The sulphides and gangue generally show crustiform and other open space filling textures.

Sediment and sulphide geochemistry

The geochemistry of Early and Late Silurian sediments and massive sulphide samples was investigated by both whole rock (XRF) and selected element (AAS) analysis[1] of 89 samples.

Early Silurian sediments

Siltstones, shales and sandstones from the Tombong Beds and Merriangaah Siltstone show compositions and element ratios very similar to those of the stratigraphically equivalent State Circle Shale, near Canberra, and to Silurian sediments from the Snowy Mountains area (Nance and Taylor 1976, Wyborn and Chappel 1983). All of these sediments have very low CaO and Na_2O contents ($<0.47\%$ and $<0.65\%$ respectively), reflecting depletion of detrital feldspar during reworking of earlier, feldspar-depleted Ordovician source sediments (Wyborn and Chappell 1983). The rocks are chemically very mature and contain a high proportion of clay relative to feldspar and mica, as indicated by $Al_2O_3/Al_2O_3+CaO+Na_2O+K_2O$ (CIA indices of 74–99, mean 80). There is no evidence for any significant input of fresh igneous detritus, although there are some small conglomerate lenses in the Tombong Beds which contain minor volcanic and coarser grained igneous clasts.

Base metal contents are very low (<100 ppm Cu+Pb+Zn), particularly when compared with values in the

[1] Analyses and element correlation matrices are available from the author on request

Table 1. Representative electron microprobe analyses of sulphides from the Clarke's Reef prospect, Quidong

Wt%	1.	2.	3.	4.	5.	6.	7.	8.	9.
Pb	n.a.	n.a.	85.92	86.40	n.a.	n.a.	n.a.	n.a.	n.a.
Zn	64.24	65.57	–	–	n.a.	n.a.	n.a.	n.a.	n.a.
Fe	1.78	1.76	–	–	46.32	46.12	46.89	59.87	60.04
Cu	0.05	–	0.04	–	0.05	–	–	–	–
As	0.07	0.05	n.a.	n.a.	0.10	–	–	0.12	0.21
S	33.01	33.69	12.57	12.83	53.54	53.99	53.51	39.58	39.88
Total	99.15	101.07	98.53	99.23	100.11	100.11	100.40	99.57	100.13
	Formulae								
Pb			1.058	1.042					
Zn	0.954	0.955	–	–					
Fe	0.031	0.030	–	–	0.993	0.981	1.006	0.868	0.844
Cu	0.001	–	0.002	–	0.001	–	–	–	–
As	0.001	0.001			0.002	–	–	0.001	0.002
S	1.000	1.000	1.000	1.000	2.000	2.000	2.000	1.000	1.000
No. of analyses	2	3	1	1	2	1	1	1	2

1–2. Sphalerite from massive sulphide vein
3–4. Galena from massive sulphide vein
5. Fractured pyrite associated with galena and sphalerite
6. Euhedral pyrite partially replaced by pyrrhotite
7. Irregular secondary pyrite replacing pyrrhotite
8. Monoclinic pyrrhotite replacing pyrite
9. Disseminated monoclinic pyrrhotite associated with pyrite and chalcopyrite

(–) not detected; n.a. not analysed; Co and Ni were analysed in pyrite and pyrrhotite but were below detection; Ag and Sb were analysed in galena and Mn in sphalerite but were also below detection. Detection limits: S 0.03%; Fe, Co, Ni,Cu 0.04%; As, Sb, Zn 0.05%; Ag 0.08%; Pb 0.5%

overlying Late Silurian rocks (Fig. 5). Other trace elements including Cr, Zr, Rb and Sr are significantly more abundant than in the Late Silurian sediments.

The Early Silurian sediments show strong positive correlation between Al, Ti, K and to a lesser extent Ca. These elements in turn show strong negative correlation with Si suggesting that they are concentrated in a matrix component separate from abundant detrital quartz. Iron, Mn, Zn, Co and Ni show moderate positive correlation, possibly due to concentration in an oxide phase such as magnetite, hematite or amorphous iron oxide in the matrix. Manganese, Zn, Co and Ni show very poor correlation with Al, Mg, K and S and are therefore not thought to be bound in chlorite, sericite or sulphides.

Late Silurian sediments

Siltstones and shales from the pyritic facies are chemically distinct from other sediments in the basin and from typical siltstones and shales (Figs. 4 and 5). They are characterised by high Mg and Fe contents, (MgO, 3–19%, mean 10% and total Fe, 2–25%, mean 9%), which reflect the abundance of chlorite and pyrite. Trends on major component diagrams (Fig. 4) are consistent with a dominant mineralogy of quartz, chlorite and variable pyrite for most of the siltstones and shales. Calcium contents are generally very low (mostly $<1\%$ CaO) reflecting the observed separation of minor carbonate into bioclastic limestone bands. Sulphur contents range from 0.15%–29% (mean 5.8% for 49 analyses), values which are considerably higher than for any other rocks in the basin. Whole rock data show very low K_2O and Na_2O contents, consistent with the generally low contents of sericite, K-bearing clay and detrital feldspar in the rocks.

Minor element data confirm the distinctive geochemical character of the pyritic siltstones and shales. Manganese contents (150–3,150 ppm, mean 1,100 ppm) are significantly higher than in sediments from the Tombong Beds, Merriangaah Siltstone and Delegate River Mudstone (70–810 ppm), although the values are not exceptionally high (cf. 650–890 ppm for average shales, Taylor and McClennan 1985). Contents of Cu, Pb and Zn are very variable but significantly higher than in other sediments, with total base metal contents varying from background values of 70–1,000 ppm up to 3% in the more pyritic sediments (Fig. 5). Many siltstones, including nonmineralised samples show enrichment in Cu relative to Pb and Zn when compared to other siltstones and shales. There is also a distinct separation of Cu from Pb in mineralised siltstones and massive and vein-type sulphides (Fig. 6). Lead tends to be more abundant in vein-type mineralisation and there is also a suggestion of larger scale zoning across the basin with high Cu and low Pb values along the western side. Nickel and Co contents (<55 ppm and <90 ppm) are similar to those of average shales and siltstones (e.g. Taylor and McClennan 1985).

Sandstones from the pyritic facies show similar major element proportions to the siltstones but are generally nonpyritic and have lower base metal contents (<400 ppm Cu + Pb + Zn).

Minor limestones and marls in the pyritic facies are mostly low in Fe, S and base metals (35–520 ppm Cu + Pb + Zn), consistent with the observed lack of sedimentary pyrite and base metal sulphides in these rocks. Magnesium

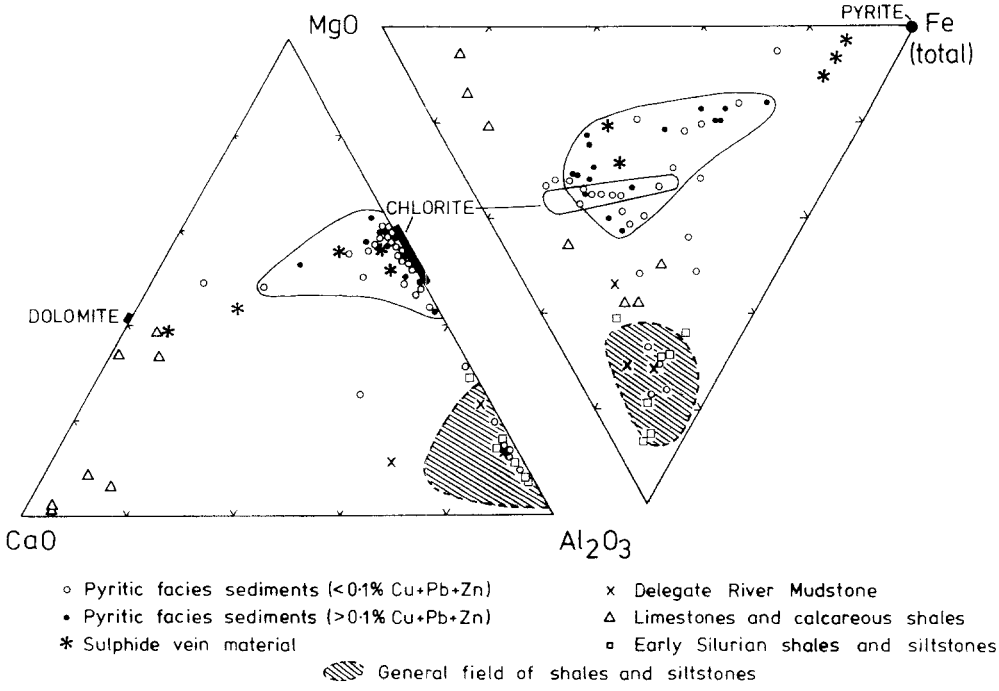

Fig. 4. Plots of some major components (summed to 100%) in the pyritic siltstones and other sediments from Quidong. Also shown is the compositional range of chlorite in these sediments (bar and small circled area). Larger circled fields show the compositional range of the metal-rich sediments. General fields for shales and siltstones are from Krauskopf (1967), Pettijohn (1975), and Taylor and McClennan (1985)

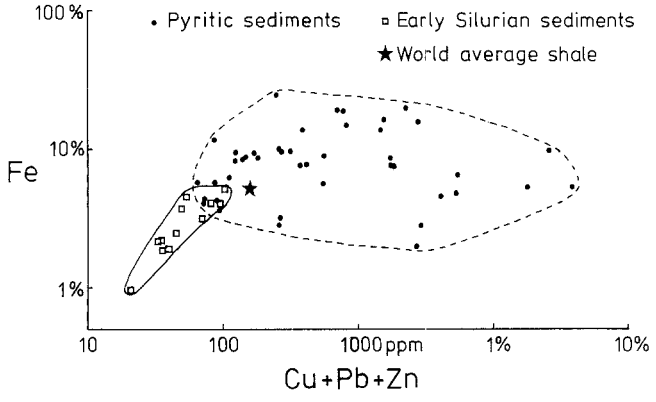

Fig. 5. Base metal and Fe contents of Early Silurian sediments and Late Silurian pyritic sediments at Quidong. Average shale values are from Krauskopf (1967) and Taylor and McClennan (1985)

contents vary with dolomite abundance and the carbonate rocks are relatively enriched in Mn.

Siltstones and shales from the overlying limestone-rich facies of the Quidong Limestone are generally less magnesian than the basal siltstones and although some are pyritic with minor base metal mineralisation, Pb, Zn and Cu contents are mostly low. These sediments are also more Ca rich indicating greater intermixing of carbonate material with the original silts and muds.

Shales from the Delegate River Mudstone at the top of the Late Silurian sequence show compositions approaching those of average shales with higher Al, Ca, K and lower Mg and Fe than the basal pyritic sediments. Base metal and S contents are very low (<150 ppm Cu+Pb+Zn, <0.28% S).

The pyritic sediments are characterised by strong positive correlation between Ca and C, and between Fe and S due to dominant concentration of these element pairs in carbonate and pyrite respectively. Magnesium and Al show moderate positive correlation reflecting their abundance in chlorite. Nickel is positively correlated with Al suggesting that it is also tied to chlorite. Cobalt displays moderate positive correlation with Fe and S, consistent with concentration of minor Co in pyrite. Lead and Zn are also positively correlated, as expected from the observed concentration of sphalerite and galena together in mineralised rocks. Copper shows its most significant correlation with Ca possibly indicating a relationship with the minor carbonate fraction. None of the base metals show strong positive correlation with S, despite the fact that they occur in sulphides, however this is undoubtedly due to the masking effect of abundant pyrite.

Sulphide bodies

Analyses of sulphide samples from Clarke's Reef show that the mineralisation is Zn- and Pb-rich but with some separate Cu-rich sections. Ratios of Pb/Zn vary from 0.31–1.16 and there is strong positive correlation of these two elements. Copper/zinc ratios vary widely and Cu and Pb show strong negative correlation, consistent with the observed separation of galena and chalcopyrite (Fig. 6). The sulphides have very low Ag contents (<20 ppm), gold values up to 0.5 ppm and As contents less than 0.8% (Brooke 1981, Brown 1983). Major element chemistry reflects the quartz, chlorite, lesser carbonate gangue. Magnesium, Al and Ni are positively correlated, again due to the occurrence of these elements in chlorite. Calcium, Mn and C are also positively correlated, suggesting concentration in carbonate gangue.

Isotopic data

Sulphur isotope ratios ($^{34}S/^{32}S$) were determined for different pyrite types, including medium to fine grained syngenetic pyrite from the pyritic sediments, coarser, recrystallised pyrite developed along fractures in these rocks, pyrite from massive sulphides at Clarke's Reef and disseminated, euhedral pyrite from a porphyry dyke intruding the lower part of the Late Silurian sequence. All the pyrite samples show $\delta^{34}S$ values between +3.4 and +9.5‰, and are similar

Table 2. Lead isotope ratios of galenas from Quidong

Sample no./Type	$^{206}Pb/^{204}Pb$	$^{207}/Pb^{204}Pb$	$^{208}Pb/^{204}Pb$	$^{207}Pb/^{206}Pb$
CRD1-10 massive sulphides	18.131	15.620	38.170	0.862
CRD4-2 veinlet galena-sphalerite	18.087	15.622	38.165	0.864
CRD4-4 veinlet galena-sphalerite	18.070	15.615	38.151	0.864
QB 43 galena-barite ore	18.091	15.625	38.167	0.864
Precision (95% Con. Lim.)	±0.010	±0.013	±0.038	±0.013

Average of 3 determinations for each sample. Analyst J.R. Richards

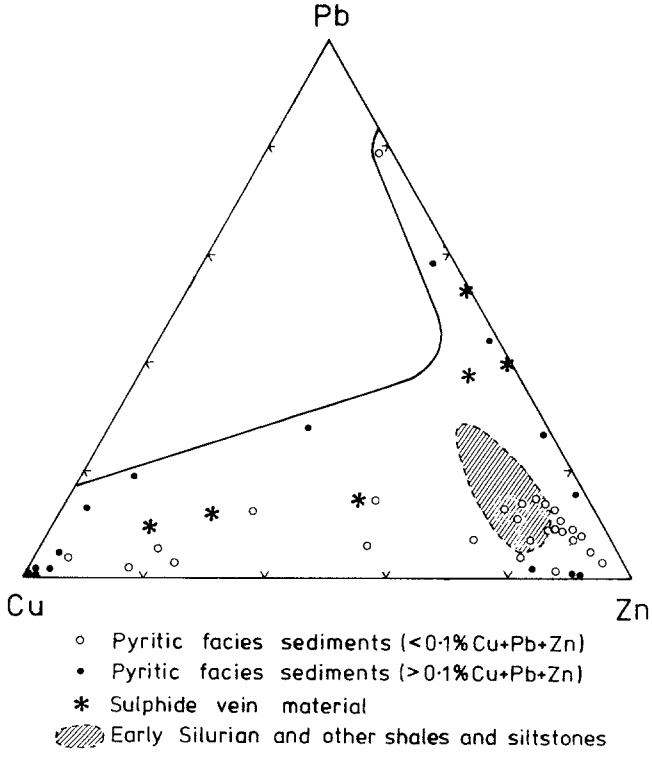

Fig. 6. Cu-Pb-Zn contents (summed to 100%) of Early Silurian sediments, pyritic sediments and massive sulphides at Quidong

to, or slightly less positive than, values for pyrite from the Late-Silurian volcanogenic sulphide deposits at Woodlawn and Captain's Flat to the north (Fig. 7). Generally the syngenetic and recrystallised pyrites show the highest positive values. All values are less positive than the accepted value for Late Silurian seawater sulphate (+26‰, Kaplan 1975).

Lead isotope determinations on three galena samples from Clarke's Reef and one sample of galena from limestone-hosted galena-barite mineralisation in the northern part of the basin, indicate a very narrow spread of Pb208/Pb204, Pb207/Pb204 and Pb206/Pb204 ratios (Table 2). The data fit the model growth curve (linear model III of Cumming and Richards 1975) and indicate "normal" type lead. The ratios also fall within the very restricted range found for galenas and massive sulphide ores in a number of Late-Silurian volcanogenic and related deposits from the Lachlan Fold Belt, including Woodlawn, Captain's Flat, Benambra and Elura (Fig. 8, Gulson 1977, 1979, 1986; Gulson and Vaasjoki 1982, Richards, pers. comm.).

Discussion

Origin of the pyritic sediments

The basal pyritic sediments at Quidong represent a geochemically distinct sedimentary facies reflecting unusual element concentrations in the basin and conditions of deposition and diagenesis which produced and preserved an abundant sulphide component. The sediments were deposited in a shallow marine environment, as indicated by the minor benthonic fauna, but probably in deeper water than the contiguous and overlying limestones. These limestones contain abundant remains of tabulate corals and calcareous algae, as well as cross-bedded sandstone lenses, reworked lag deposits and reefal structures, suggesting a shallow water, high energy environment (i.e. within the photic and tidal zones).

The mineralogy and geochemistry of the pyritic sediments suggest that they were formed from three major components. These included: (a) a quartz-rich terrigenous component; (b) Mg-bearing clay or chlorite; and (c) sedimentary/diagenetic or hydrothermal pyrite.

The terrigenous component was probably derived largely from the underlying flysch rocks as suggested by the occurrence of quartzite clasts from the Tombong Beds in conglomerates at the base of the pyritic facies, the marked lack of detrital feldspar and presence of similar accessory minerals in both rock groups.

A significant Mg-bearing clay component is indicated by the high Mg and Al contents of the pyritic siltstones and shales. There is no obvious terrigenous source for this material and it is unlikely that Mg-rich composition were developed by regional alteration processes after deposition. Restriction of highly magnesian sediments to a particular facies, in sharp contact with non-chloritic sediments, would rule out large scale Mg metasomatism during regional metamorphism, although some minor remobilisation of Mg and formation of vein chlorite and dolomite did occur at this stage. It is therefore suggested that Mg-bearing clays (e.g., Mg-rich montmorillonite) may have been precipitated from hydrothermal fluids discharged into the basin at the time of deposition or possibly formed from the alteration of fine ash added to the basin sediments by volcanic activity. Similar processes have been suggested for the origin of chloritic and Mg-rich rocks associated with stratiform sulphide deposits from a number areas (e.g., Stanton 1976, Petersen and Lambert 1979, Bernard et al. 1982, McLeod and Stanton 1984). The presence of cherty exhalites and minor tuff bands in the sediments at Quidong clearly indicates some concomitant volcanic and hydrothermal activity. Alteration of early formed clays to chlorite could have occurred during diage-

nesis or low grade metamorphism and possible mechanisms for this process are reviewed by McLeod and Stanton (1984).

Pyrite textures, including framboids, bedding-parallel concentrations of fine euhedral grains and pyrite concretions, point to a sedimentary or diagenetic origin for much of the sulphide in the siltstones and shales. These iron sulphides probably formed by reaction of Fe in clays or oxides with reduced sulphur either provided by bacterial seawater sulphate reduction or added from an exhalative source. Direct precipitation of iron sulphides from hydrothermal exhalations is also a possibility, particularly for some of the highly pyritic sediments (cf. Honnorez et al. 1973). Anoxic conditions at or below the sediment seawater interface would have been required to allow early formed, sedimentary iron sulphides to be preserved and converted to pyrite during diagenesis. Drever (1971) has demonstrated that under such anoxic conditions it is possible to extract Fe from clays to form sulphide, with Mg replacing Fe in the clay mineral structure. In addition to providing Fe, this process could also help explain the association of Mg-rich clays, and ultimately chlorite, with pyrite in the Quidong sediments. The trend towards more Mg-rich chlorite compositions with increasing pyrite content in the sediments is also consistent with this type of aqeous extraction of Fe from clays by reduced sulphur (cf. McLeod and Stanton 1984).

Origin of the massive sulphide deposits

There are two possible modes of origin for the small bodies of massive, stratabound and vein-type sulphides. The deposits may have formed by fluid assisted remobilisation of metals and sulphur into structural sites from the sulphidic sediments, for example during diagenetic dewatering or deformation and low grade regional metamorphism. Alternatively the sulphide bodies may have formed around and within vents which controlled hydrothermal fluid discharge into the basin during and after sediment deposition. The known massive sulphide bodies generally occur along or close to faults, or within areas of major faulting near the base of the Late Silurian sequence. These faults are high angle structures which commonly extend into the Early Silurian and Ordovician basement as well as into the overlying parts of the sequence (Fig. 2). Some appear to have been active prior to folding and low-grade regional metamorphism in the basin, and others have controlled the emplacement of porphyry dykes. Faults that were active in the early stages of deposition could have provided channelways for sea water circulation or discharge of deeper magmatic fluids into the basin. Continued fluid movement along major structures after deposition of the pyritic facies could account for the development of discordant, sulphide veins and the minor galena-barite mineralisation and accompanying dolomitisation in overlying limestones. Ore textures at Clarke's Reef indicate multi-stage epigenetic deposition of sulphides and barite as well as some post-depositional deformation.

Fluid sources

The S isotope data for pyrite in the sediments and massive sulphide deposits are consistent with sulphide derivation by partial reduction of Silurian seawater sulphate. The data support either biogenic reduction or inorganic reduction, for example during thermally driven seawater circulation

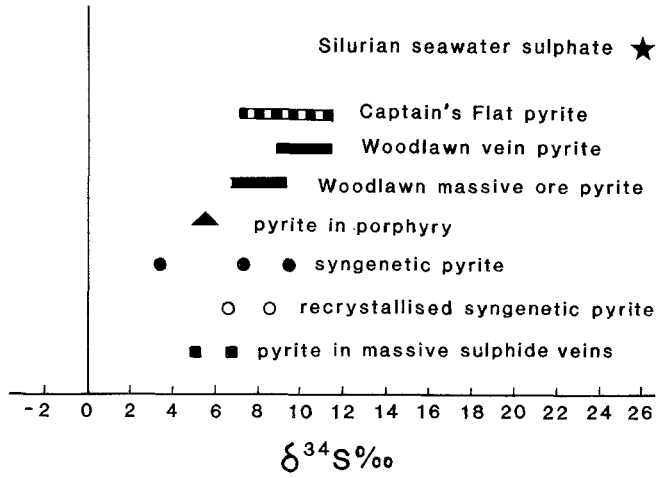

Fig. 7. S isotope data for Quidong pyrites compared with similar data from the Woodlawn and Captain's Flat volcanogenic sulphide deposits (Ayers et al., 1979; S. Sun, pers comm.). Values are relative to CDT, analytical precision is ±0.2‰

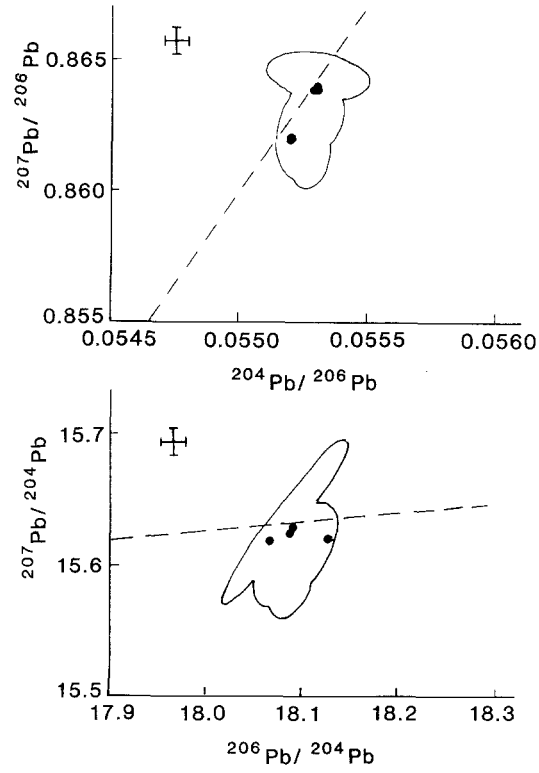

Fig. 8. Pb isotope data from Quidong compared with ore Pb data from Woodlawn, Captain's Flat and Benambra (95% confidence ellipses; Gulson, 1986). Dashed lines are Pb evolution curves of Cumming and Richards (1985), error bars are ±2 δ

prior to exhalation onto the sea floor. Biogenic reduction would imply a shallow, restricted basin largely closed to sulphate, as straight biogenic sulphate reduction in an open system would have resulted in more negative $\delta^{34}S$ values. Such closed system conditions are not generally indicated by the sedimentary lithologies. The isotope data do not support a direct magmatic S source, however the possibility of a magmatic component, for example in exhaled fluids derived from underlying felsic magmas, can not be ruled out. The

isotope ratio of pyrite in high level porphyry dykes, probably derived from such felsic magmas, overlaps with the lower range of isotopic ratios in the sediments (Fig. 7).

The marked similarity between Pb isotope ratios in galena from Quidong and Pb-rich ores from a number of massive sulphide deposits in the Lachlan Fold Belt (Fig. 8, Gulson 1986) suggests a common or similar, homogeneous source for the Pb in all these deposits. The near uniform isotopic ratios for the volcanogenic and related deposits have previously been interpreted as indicating a common Pb source, probably involving crustal material of similar composition to the associated volcanics (Gulson 1977, 1986). The ratios are also distinct from those for the Ordovician basement rocks (e.g., at Woodlawn, Gulson 1979) and this, together with the very low Pb contents of the Ordovician metasediments, would preclude these rocks as a likely Pb source. At Quidong the Early Silurian sediments also have very low Pb contents and likewise would not represent a suitable source for Pb. The Pb for all the Late Silurian deposits could have been derived from deeper crustal material during widespread partial melting and magma generation in the Mid Silurian to Early Devonian. These processes gave rise to large volumes of felsic magmas and associated volcanics, and Pb plus other metals could have been sourced directly from fluids associated with the magmas or, in some areas, leached from the resulting volcanics by seawater circulation.

Conclusions

The sulphide-rich sediments and stratabound sulphide deposits at Quidong can both be explained by hydrothermal solution activity during and after deposition of the Late Silurian sequence. Development of the Quidong basin and deposition of shallow marine sediments coincided with initiation of major magmatic and volcanic activity, uplift and tectonic extension throughout the southern Lachlan Fold Belt (cf. Powell 1986). The Quidong area appears to have been distal from the major volcanic centers, however the presence of thin tuff layers, exhalites and shallow intrusions, particularly in the basement, indicate some thermal activity in the area at this time. Hydrothermal exhalations introduced abundant sulphide and minor base metals into the early basin sediments and produced small stratabound and vein-type sulphide deposits with higher grade base metals, in and around exhalative centers (e.g. Clarke's Reef). Mineralisation continued after deposition of the overlying rocks and may have involved some remobilisation from syngenetic sulphides. Isotopic data for the sediments and massive sulphides are best explained by mixing of reduced sulphur, largely derived by sea water sulphate reduction, with metal-bearing fluids, probably generated by deeper crustal melting and magmatic processes. The geochemistry of the underlying Early Silurian sediments indicates that they were not a likely source for the metals and S, further suggesting that metal-bearing fluids were derived from lower in the crust.

Proximal, volcanogenic massive sulphide deposits and volcanic hosted, disseminated and stringer-vein deposits are well known from Late Silurian sequences in the southern Lachlan Fold Belt (e.g., Gilligan 1974, Degeling et al. 1986, Ramsay and Vandenberg 1986). The base metal enriched, sulphidic sediments and associated stratabound sulphide concentrations at Quidong represent a hitherto unrecognised style of more distal mineralisation in rocks of this age within the Lachlan Fold Belt. This style of mineralisation shows some similarities with sediment hosted Pb-Zn mineralisation of the Alpine and Irish types (Sangster 1976, Maynard 1983). Such deposits typically occur in shallow marine basins which were tectonically active during and after sediment deposition. The basin sequences are dominated by bioclastic and reefal limestones together with calcareous shales and sandstones, and many also contain minor volcanic rocks indicating contemporaneous volcanism. Other common features include the occurrence of stratiform sulphides, together with stratabound, vein and replacement style massive sulphides, close association of mineralisation with faults, development of tectonically controlled vein mineralisation in surrounding rocks, evidence for remobilisation of sulphides, occurrence of anomalous metal values in pre- and post-ore sediments and the presence of exhalative chert and barite (Schulz 1964, Maucher and Schneider 1967, Russell 1975, Brigo et al. 1977, Riedel 1980, Hitzman and Large 1986). Many of these features are present at Quidong and it is suggested that the mineralisation here represents an Eastern Australian analog of the Irish-Alpine type spectrum. Similar deposits probably exist in other areas of the Lachlan Fold Belt where distal, exhalative processes operated during the Siluro-Devonian volcanism. Mineralisation in the Irish and Alpine deposits has variously been ascribed to syngenetic and/or epigenetic deposition from fluids derived by downward penetration and convective circulation through basement rocks of modified, highly saline seawater (e.g., Russell et al. 1981, Köppel and Schroll 1988), syngenetic and epigenetic deposition from volcanic, hydrothermal fluids (Schneider 1964, Schulz 1964, Maucher and Schneider 1967) and deposition or remobilisation by formational fluids (Berce 1967, Bechstadt 1978, Lydon 1986). Features at Quidong which depart from those in most Irish-Alpine deposits include the concentration of mineralisation in non-calcareous sediments, the very low Ag content of the sulphides compared with Irish type deposits and relatively high Cu content compared with most Alpine and some Irish deposits, heavier S isotopes and presence of isotopically "normal" lead (cf. Caulfield et al. 1986, Klau and Mostler 1986, Köppel and Schroll 1988). Some of these differences may reflect a larger, or more direct, volcanic-exhalogenic component in the history of the Quidong mineralisation.

Acknowledgements. I sincerely thank Dr. J. R. Richards, Research School of Earth Sciences, Australian National University and Dr. S. Sun from the Bureau of Mineral Resources for carrying out the Pb and S isotope determinations respectively. I also thank S. Trigg and M. Fenton for some XRF analyses. Electron microprobe analyses were performed at the Geology Department, University of Melbourne. The Western Mining Corporation provided some logistic support for the study and undertook the S and C determinations. Thanks are also due to W.J.L. Brooke and R. Barratt from WMC for assistance with drill core sampling and discussions on the Quidong area. Mr. B. Stevenson from Quidong station kindly allowed access to his property during the field work. The study was funded by a C.C.A.E. research grant.

References

Ayers, D.E., Burns, M.S., Smith, J.W.: Sulphur isotope study of the massive sulphide orebody at Woodlawn, New South Wales. J. Geol. Soc. Aus. 26:197–201 (1979)

Bechstadt, T.: The lead-zinc deposit of Bleiberg-Kreuth (Carinthia, Austria): Palinspastic situation, paleogeography and ore mineralization. Proc. 3rd ISMIDA Verh. Geol. B-A: 221–235 (1978)

Berce, B.: The stratiform lead-zinc deposits bordering the eastern alps and their genetic elements. In: Genesis of Stratiform Lead-Zinc-Barite-Fluorite Deposits in Carbonate Rocks, J.B. Brown Ed., Econ. Geol. Monogr. 3:126–132 (1967)

Bernard, A.J., Degallier, G., Soler, E.: The exhalative sediments linked to the exhalative massive sulphide deposits: a case study of European occurrences. In: Amstutz, G.C., El Goresy, A., Frenzel, G., Kluth, C., Moh, G., Wauschkuhn, A., Zimmermann, R.A., Eds., pp. 553–564. Berlin-Heidelberg-New York: Springer 1982

Brigo, L., Kostelka, L., Omenetto, P., Schneider, H.J., Schroll, E., Schulz, O., Strucl, I: Comparative reflections on four Alpine Pb-Zn Deposits. In: Time and Stratabound Ore Deposits, Klemm, D.D., Schneider, H.J., Eds., pp. 273–293. Berlin-Heidelberg-New York: Springer 1977

Brown, C.H.: Final report EL 1147–1148, Merriangaah Peak – Quidong area, Bombala district. Unpubl. Rep. Geol. Surv. N.S.W., GS 1983/248 (1983)

Brooke, W.J.L.: Exploration reports EL's 1147 and 1148, Merriangaah Peak – Quidong area, Bombala district. Unpubl. Reps Geol. Surv. N.S.W., GS 1981/191 (1981)

Brunker, R.L., Offenberg, A.C., West, J.L.: Monaro 1:500,000 Geological Sheet. Sydney: Geological Survey N.S.W. 1971

Caulfield, J.B.D., LeHurray, A.P., Rye, D.M.: A review of lead and sulphur isotope investigations of Irish sediment-hosted base metal deposits with new data from the Keel, Ballinalach, Moyvaughly and Tatestown deposits. In: Andrew, C.J., Crowe, R.W.A., Finlay, S., Pennell, W.M., and Pyne, J.F., Eds., pp. 591–615. Dublin: Irish Assoc. for Economic Geology 1986

Crook, K.A.W., Bien, J., Hughes, R.J., Scott, P.H.: Ordovician and Silurian history of the southeastern part of the Lachlan Geosyncline. J. Geol. Soc. Aus. 20:113–138 (1973)

Cumming, G.L., Richards, J.R.: Ore lead isotope ratios in a continuously changing earth. Earth Planet. Sci. Lett. 28:155–171 (1975)

Deer, W.A., Howie, R.A., Zussman, J.: An Introduction to the Rock Forming Minerals. London: Longmans 1967

Degeling, P.R., Gilligan, L.B., Scheibner, E., Suppel, D.W.: Metallogeny and tectonic development of the Tasman Fold Belt system in New South Wales. Ore Geology Reviews, 1:259–313 (1986)

Drever, J.: Magnesium-iron replacement in clay minerals in anoxic marine sediments. Science, 172:1334–1336 (1971)

Gilligan, L.B.: Cowra-Yass Synclinorial Zone; Captain's Flat Synclinorial Zone. In: The Mineral Deposits of New South Wales, Markham, N.L., Basden, H., Eds., pp. 218–230 and 294–306. Sydney: Geological Survey N.S.W. (1974)

Gulson, B.L.: Isotopic and geochemical studies on crustal effects in the genesis of the Woodlawn Pb-Zn-Cu deposit. Contrib. Mineral Petrol. 65:227–242 (1977)

Gulson, B.L.: A lead isotope study of the Pb-Zn-Cu deposit at Woodlawn, New South Wales. J. Geol. Soc. Aus. 26:203–208 (1979)

Gulson, B.L.: Lead Isotopes in Mineral Exploration. Developments in Economic Geology, 23. Amsterdam: Elsevier 1986

Gulson, B.L., Vaasjoki, M.: Lead isotopes in geochemical exploration. In: Geochemical Exploration in Deeply Weathered Terrain, Smith, R.E., Ed., pp. 145–151. Sydney: CSIRO Division of Mineralogy (1982)

Hitzmann, M.W., Large, D.: A review and classification of the Irish Carbonate-hosted base metal deposits. In: Geology and Genesis of Mineral Deposits in Ireland, Andrew, C.J., Crowe, R.W.A., Finlay, S., Pennell, W.M., and Pyne, J.E., Eds., pp. 217–238. Dublin: Irish Assoc. for Economic Geology (1986)

Honnorez, J., Honnerez-Guerstein, B., Vallett, J., Wauschkuhn, A.: Present day formation of an exhalative sulfide deposit at Vulcano (Thyrrhenian Sea), Part II: Active crystallization of fumarolic sulfides in the volcanic sediments of the Baia di Levante. In: Ores in Sediments, Amstutz, G.C., Bernard A.J., Eds., pp. 139–166 Berlin-Heidelberg-New York: Springer 1973

Kaplan, I.R.: Stable isotopes as a guide to biogeochemical processes. Proc. R. Soc. London B 189:181–211 (1975)

Klau, W., Mostler, H.: On the formation of Alpine Middle and Upper Triassic Pb-Zn deposits, with some remarks on Irish carbonate-hosted base metal deposits. In: Andrew, C.J., Crowe, R.W.A., Finlay, S., Pennell, W.M., and Pyne, J.F., Eds., pp. 663–675. Dublin: Irish Assoc. for Economic Geology 1986

Köppel, V., Schroll, E.: Pb-isotope evidence for the origin of lead in strata-bound Pb-Zn deposits in Triassic carbonates of the eastern and southern Alps. Mineral. Deposita 23:96–103 (1988)

Krauskopf, K.B.: Introduction to Geochemistry. New York: McGraw Hill (1967)

Link, A.G.: Age and correlation of the Siluro-Devonian strata in the Yass Basin, New South Wales. J. Geol. Soc. Aus. 16:711–722 (1970)

Lydon, J.W.: Models for the generation of metalliferous hydrothermal systems within sedimentary rocks, and their applicability to the Irish Carboniferous Zn-Pb deposits. In: Geology and Genesis of Mineral Deposits in Ireland, Andrew, C.J., Crowe, R.W.A., Finlay, S., Pennell, W.M., and Pyne, J.F., Eds., pp. 552–577. Dublin: Irish Assoc. for Economic Geology (1986)

McLeod, R.L., Stanton, R.L.: Phyllosilicates and associated minerals in some Paleozoic stratiform sulphide deposits of southeastern Australia. Econ. Geol. 79:1–22 (1984)

McQueen, K.G., Taylor, G., Brown, M.C.: The Cambalong Complex: A new metamorphic complex in southeastern New South Wales. Proc. Lin. Soc. N.S.W. 108:287–292 (1986)

Maucher, A., Schneider, H.J.: The Alpine lead-zinc ores. In: Genesis of Stratiform Lead-Zinc-Barite-Fluorite Deposits in Carbonate Rocks, J.S. Brown Ed., Econ. Geol. Monogr. 3:71–81 (1967)

Maynard, J.B.: Geochemistry of Sedimentary Ore Deposits, Berlin-Heidelberg-New York: Springer 1983

Nance, W.B., Taylor, S.R.: Rare earth element patterns and crustal evolution 1. Australian post-Archaean sedimentary rocks. Geochim. Cosmochim. Acta 40:1539–1551 (1976)

Peterson, M.D., Lambert, I.B.: Mineralogical and chemical zonation around the Woodlawn Cu-Pb-Zn ore deposit, southeastern New South Wales. J. Geol. Soc. Aus. 26:169–186 (1979)

Pettijohn, F.J.: Sedimentary Rocks, 3rd Ed. New York: Harper and Row (1975)

Pickett, J.: The Silurian System in New South Wales. Geological Survey of N.S.W. Bulletin, 29, Sydney (1982)

Pogson, D.J.: Geological map of New South Wales, Scale 1:1,000,000. Sydney: Geological Survey N.S.W. (1972)

Powell, C. McA.: Silurian to mid-Devonian – dextral transtensional margin. In: Phanerozoic History of Australia, J.J. Veevers Ed., pp. 309–329. Oxford: Oxford Univ. Press (1986)

Ramsay, W.R.H., Vandenberg, A.H.M.: Metallogeny and tectonic development of the Tasman Fold Belt system in Victoria. Ore Geology Reviews, 1:213–257 (1986)

Richardson, S.J.: Geology of the Michelago 1:100,000 Sheet 8726. Sydney: Geological Survey N.S.W. (1979)

Riedel, D.: Ore structures and genesis of the lead-zinc-deposit, Tynagh, Ireland. Geol. Rdsch. 69:361–383 (1980)

Russell, M.J.: Lithogeochemical environment of the Tynagh base metal-deposit, Ireland, and its bearing on ore deposition. Trans. Inst. Min. Metall. 84B:128–133 (1975)

Russell, M.J., Solomon, M., Walshe, J.L.: The genesis of sediment-hosted, exhalative zinc-lead deposits. Mineral. Deposita 16:113–127 (1981)

Sangster, D.F.: Carbonate-hosted lead-zinc deposits. In: Handbook of Strata-bound and Stratiform Ore Deposits, K.H. Wolf Ed., Vol. 6, pp. 447–456. Amsterdam: Elsevier 1976

Scheibner, E.: A plate tectonic model of the Palaeozoic tectonic history of New South Wales. J. Geol. Soc. Aus. 20:405–426 (1973)

Schneider, H.J.: Facies differentiation and controlling factors for the depositional lead-zinc concentration in the Ladinian geosyn-

cline of the eastern Alps. In: Sedimentology and Ore Genesis, Amstutz, G.C., Ed., pp. 29–46. Amsterdam: Elsevier 1964
Schulz, O.: Lead-zinc deposits of the calcareous Alps as an example of submarine-hydrothermal formation of mineral deposits. In: Sedimentology and Ore Genesis, Amstutz, G.C., Ed., pp. 47–52. Amsterdam: Elsevier 1964
Stanton, R.L.: Petrochemical studies of the ore environment at Broken Hill, New South Wales – Part 2. Trans. Inst. Min. Metall. 85B:118–131 (1976)
Taylor, S.R., McClennan, S.M.: The Continental Crust: Its Composition and Evolution. Oxford: Blackwell 1985
Wyborn, L.A.I., Chappell, B.W.: Chemistry of the Ordovician and Silurian greywackes of the Snowy Mountains, southeastern Australia: An example of chemical evolution of sediments with time. Chemical Geology 39:81–92 (1973)

Received: August 2, 1988
Accepted: November 22, 1988

Book review

I. L. Komov, A. N. Lukashev, A. V. Koplus: Geochemical Methods of Prospecting for Non-metallic Minerals. Utrecht: VNU Science Press (now known as VSP International Science Publishers), 1987. Translated from the Russian by V. I. Sverdlov. 241 pp. 13 tables. 29 fig., (ISBN 90-6764-081-6), hard cover, DM 274,— (approximately $ 150)

The title of this book attracts attention because it is the only compilation in which geochemical methods are used in exploration for non-metallic resources. The book considers 39 non-metallic commodities of which eleven are gems or semi-precious stones; these are diamond, beryl (including emerald), topaz, corundum (sapphire, ruby), rhodonite, malachite, chrysoprase (but not other varieties of quartz, such as amythest or citrine), turquoise, nephrite, jadeite and lazurite. The remaining 28 commodities include graphite, asbestos, muscovite, phlogopite, rock crystal, Iceland spar, apatite, phosphorite, boron, barite, fluorite, sulphur, salts (including halite, sylvite, carnallite and epsomite), natural soda, gypsum and anhydrite, limestone and dolomite, magnesite, wollastonite, brucite, talc, jadeite, feldspars and pegmatities, vermiculite, vein quartz and quartzites, sand and gravel, clays, perlite (including pumice and volcanic glass), siliceous rocks, and rocks used as building stones. The vast majority of the above commodities are covered in three pages or less. Only exploration methods for diamond, beryl, topaz, asbestos, muscovite, rock crystal, Iceland spar, apatite, phosphorite, boron, barite and sulphur receive more than five printed pages.

The discussions of most of the commodities are treated in a similar manner starting with their geological occurrences (in some cases, these can be varied and numerous) in which geochemical pathfinder (indicator) elements and associated minerals are identified. To this point, the presentations are what one would expect in a book on economic geology of non-metallic minerals. This is followed by discussions of the best geochemical methods for the detection of the pathfinder elements and minerals in the most appropriate type(s) of geochemical sampling media, e.g. soils, stream sediment, waters, rocks and vegetation. Other topics, e.g. the extent of haloes and vertical zonality, are discussed where relevant. The book contains 50 references all but two of which are from the Soviet literature. Thirty-three of the references have publication dates from 1973 to 1977. The most recent references are to three papers which appeared in 1978. There is no index. The original Russian edition appears to have been published in 1982 (see Chem. Abstr. 97, 185856 c), although nowhere is this stated in this English version.

In reviewing any book a reviewer must be fair to both the authors as well as to the potential audience. In the case of the former, I have positive feelings with respect to the competence of the authors based on their in-depth discussion of the fundamentals of those commodities in which they appear to be most interested (those listed above which cover more than five printed pages). By compiling this book they were clearly performing a service to the U.S.S.R. where the search for non-metallic resources involves the use of geochemical methods in the total exploration program.

From the point of view of the potential buyer and user of this English translation, I am generally negative for the following reasons. First, the book is out of date and represents the state-of-the-art as it was known in the U.S.S.R. at least a decade ago. Second, only a few of the commodities considered in this book are actively being sought outside the U.S.S.R. today for which the geochemical methods described in this book are likely to be practical. Third, I would expect most practicing economic geologist and geochemists concerned with non-metallic minerals to know much of the material covered. Fourth, in many places the translation is very "rough" and the terminology translated directly from the Russian is infamiliar; further along these editorial lines I cannot remember ever seeing a book with as many typographical errors. Fifth, the cost of this book is extremely high by comparison with many other books which will be more valuable.

A. A. Levinson (Calgary)